$M_2As_2O_7(H_2O)_2$ (M = Co or Ni): Hydrous Diarsenates with an Intersecting Tunnel Structure†

Sue-Lein Wang,* Jia-Cherng Horng and Yan-Huang Lee
Department of Chemistry, National Tsing Hua University, Hsinchu, Taiwan 30043, ROC

Two new hydrous diarsenates, $M_2As_2O_7(H_2O)_2$ (M = Co or Ni), have been synthesized hydrothermally and structurally characterized by single-crystal X-ray diffraction. The cobalt compound was further defined by thermal analysis and magnetic susceptibilities. They are the first examples of the hydrous form of divalent transition-metal diarsenates. Both compounds crystallize in the monoclinic space group $P2_1/n$, with a = 6.525(2), b = 14.200(5), c = 7.618(2) Å, β = 94.72(2)°, Z = 4 and R = 0.0246 for 1369 unique reflections for $Co_2As_2O_7(H_2O)_2$ and a = 6.459(2), b = 14.033(4), c = 7.543(2) Å, β = 94.24(2)°, Z = 4 and R = 0.0272 for 952 unique reflections for $Ni_2As_2O_7(H_2O)_2$. The two compounds are isostructural. The framework consists of infinite chains of MO_6 octahedra sharing either *trans* or skew edges along the [10$\bar{1}$] direction. Adjacent chains are linked by As_2O_7 groups to form wavy sheets parallel to the (101) plane. Sheets are further connected by diarsenate anions to form a three-dimensional architecture with intersecting tunnels running along the [100] and [001] directions. Water oxygens are bonded to cobalt atoms with the hydrogen atoms directed into the tunnels. The structures are compared with those of $Co_2As_2O_7$ and $CaCo_3(P_2O_7)_2$.

Recently many new transition-metal phosphate compounds such as $AFe_5(PO_4)_5(OH)\cdot H_2O$ (A = Ca or Sr),[1a] $K_2[(VO)_2V(PO_4)_2(HPO_4)(H_2PO_4)(H_2O)_2]$[1b] $Cd_5V_3P_6O_{25}$[1c] and $A'H[Zn(PO_4)]_2$ (A' = Na or Cs)[1d] have been synthesized and structurally characterized. These phosphates show a variety of new structural types with cage, tunnel or layer structures. The synthetic approaches were two-fold, namely solid-state reactions and hydrothermal methods. The latter method is particularly useful in growing single crystals. In contrast, much less structural work on transition-metal arsenates has been reported. Recently we have undertaken an investigation of transition-metal arsenates and have synthesized several new compounds in the A–V–As–O and A–Fe–As–O systems.[2–5] In an attempt to expand this research to other transition metals, two new diarsenates, $Co_2As_2O_7(H_2O)_2$ and $Ni_2As_2O_7(H_2O)_2$ were obtained. To our knowledge, only a few structurally well characterized transition-metal diarsenates have been reported. For example, α-$TiAs_2O_7$ and β-$TiAs_2O_7$[6] were synthesized by high-temperature hydrothermal methods and characterized by single-crystal X-ray diffraction techniques and $Co_2As_2O_7$,[7] $Ni_2As_2O_7$[7] and $Mn_2As_2O_7$[7,8] were synthesized *via* solid-state reactions and structurally characterized by power diffraction methods. They are anhydrous diarsenates. Compounds in which water and diarsenate groups co-exist are rare. In this paper, we report the synthesis, single-crystal structure, thermal analysis and magnetic susceptibility studies of the first examples of hydrous divalent transition-metal diarsenates, $Co_2As_2O_7(H_2O)_2$ and $Ni_2As_2O_7(H_2O)_2$.

Experimental

Syntheses.—Reagent-grade $Co(OH)_2$, LiOH, NiO and 80% H_3AsO_4, obtained from Merck, were used as received. A purple crystalline product was obtained by heating a mixture of $Co(OH)_2$ (1.2 g), 80% H_3AsO_4 (6 cm^3) and water (6 cm^3) in a Teflon-lined autoclave (23 cm^3) at 230 °C for 4 d followed by slow cooling to room temperature at 5 °C h^{-1}. The product was filtered off, washed with water, rinsed with ethanol and dried in a desiccator at ambient temperature. The product contained purple rod-like crystals of $Co_2As_2O_7(H_2O)_2$. Its bulk X-ray powder diffraction pattern compared very well with that calculated from the single-crystal data. Energy-dispersive X-ray fluorescence analysis on a purple crystal showed that the Co : As mole ratio was 1.035 : 1, which is in accord with the structural analysis result (see below).

For the preparation of $Ni_2As_2O_7(H_2O)_2$, NiO (0.3743 g), LiOH (0.1204 g), 80% H_3AsO_4 (2.5 cm^3) and water (10.5 cm^3) were heated under the same conditions as those for the cobalt compound. Powder X-ray diffraction of the bulk product indicated that a single-phase product was also obtained.

Single-crystal X-Ray Analysis.—Many crystals were examined before a satisfactory one was obtained. Two crystals of dimensions 0.15 × 0.14 × 0.44 mm for $Co_2As_2O_7(H_2O)_2$ **1** and 0.05 × 0.07 × 0.2 mm for $Ni_2As_2O_7(H_2O)_2$ **2** were selected for indexing and intensity data collection on a Nicolet R3m/V diffractometer using Mo-Kα radiation. Axial oscillation photographs along the three axes were taken to check the symmetry properties and unit-cell parameters. Octants h, k, $\pm l$ were collected for both compounds. Of the 1956 (1462) reflections collected 1369 (952) unique reflections were considered observed [$I \geqslant 3.0\sigma(I)$] after Lorentz polarization and empirical absorption corrections for compound **1** (**2**). Correction for absorption effects was based on φ scans of a few suitable reflections with χ values close to 90° using the program XEMP from the SHELXTL PLUS program package.[9] Maximum, minimum transmission factors = 0.741, 0.918 and 0.624, 0.808 for compound **1** and **2**, respectively. On the basis of the systematic absences the space groups for both compounds were determined to be $P2_1/n$. Direct methods were used to locate the metal, arsenic and a few oxygen atoms with the remaining non-hydrogen atoms being found from successive difference maps. The hydrogen atoms were located from a Fourier-difference map calculated at the final stage of structure analysis. The final cycles of refinement, including the atomic coordinates and anisotropic thermal parameters for all non-hydrogen atoms and fixed atomic coordinates and isotropic thermal parameters for the hydrogen atoms, converged at R = 0.0246 and R' = 0.0384 for **1** and R = 0.0272 and

† *Supplementary data available:* see Instructions for Authors, *J. Chem. Soc., Dalton Trans.*, 1994, Issue 1, pp. xxiii–xxviii.

R' = 0.0307 for **2**. In the final difference map the deepest holes were −0.65 and −0.87 and the highest peaks 0.83 and 0.95 e Å^{-3} for compound **1** and **2**, respectively. Corrections for secondary extinction and anomalous dispersion were applied. Neutral-atom scattering factors were used. Structure solution and least-squares refinements were performed on a DEC VAX 4000/VLC workstation using the SHELXTL PLUS programs.

Additional material available from the Cambridge Crystallographic Data Centre comprises H-atom coordinates, thermal parameters and remaining bond lengths and angles for both compounds.

Thermal Analysis.—Thermogravimetric analysis (TG), using a Seiko SSC-5000 thermogravimetric analyser, was performed on a powder sample of $Co_2As_2O_7(H_2O)_2$ in flowing N_2 with a heating rate of 5 °C min^{-1}. The TG curve showed only one step of weight loss at *ca.* 420 °C, which was attributed to the loss of two water molecules. The observed weight loss (8.4%) is in good agreement with the calculated value (8.66%). In order to characterize the dehydrated product, an experiment was performed in which both the cobalt and nickel compounds were heated at 500 °C for 24 h. Powder X-ray diffraction patterns of the products of the heat treatment indicate that they are probably a mixture of low- and high-temperature phases of $Co_2As_2O_7$ (or $Ni_2As_2O_7$).

Magnetic Measurements.—A powder sample of $Co_2As_2O_7(H_2O)_2$ (186.77 mg) was used to collect variable-temperature magnetic susceptibility data from 2 to 300 K in a magnetic field of 3 kG (0.3 T) using a Quantum Design SQUID magnetometer. As suggested by Selwood,[10] diamagnetic contributions for Co^{2+}, As^{5+} and O^{2-} were estimated and subtracted from the experimental susceptibility data to obtain the molar susceptibility (χ_M) of the compound.

Results and Discussion

The crystallographic data are listed in Table 1, atomic coordinates in Table 2 and selected bond distances and bond-valence sums[11] in Table 3. The bond-valence sums indicate that both the cobalt and nickel atoms are divalent, the arsenic atoms pentavalent, O(2) and O(5) a little undersaturated (1.67 and 1.76 valence units), and all the other oxygens have values close to 2. The values for O(2) and O(5) indicate that they are involved in hydrogen bonding (see below). All atoms are at general positions. Both the cobalt and nickel atoms are six-co-ordinated and the arsenic atoms four-co-ordinated. In the following, only the structure of $Co_2As_2O_7(H_2O)_2$ will be discussed as the two compounds are isostructural.

The framework of $Co_2As_2O_7(H_2O)_2$ consists of infinite chains of edge-sharing CoO_6 octahedra linked by As_2O_7 groups to form a three-dimensional architecture which consists of intersecting tunnels running along the [100] and [001] directions (Fig. 1). The structure is different from that of the anhydrous diarsenate, $Co_2As_2O_7$, which is found in two polymorphs: a low-temperature α phase and a high-temperature β phase. The β phase adopts the thorvetite ($Sc_2Si_2O_7$) structure[12] with a linear As–O–As group. The structure of the α phase has not yet been reported. However, its powder X-ray diffraction pattern resembles that of the phosphate analogue, α-$Co_2P_2O_7$,[13] the structure of which is a small modification of the thorvetite with a bent P–O–P linkage. Both polymorphs contain sheets of CoO_6 octahedra sharing all possible skew edges. All oxygen atoms in the octahedra come from diarsenate (or diphosphate) groups. In contrast in $Co_2As_2O_7(H_2O)_2$ each cobalt atom is co-ordinated by five arsenate oxygen atoms and one water oxygen. The incorporation of a water molecule in the co-ordination sphere hinders the 'fusion' among the octahedra and thus results in chains rather than sheets of CoO_6 octahedra in the hydrous diarsenates.

In $Co_2As_2O_7(H_2O)_2$, the zigzag infinite chains parallel to the [10$\bar{1}$] direction [Fig. 2(*a*)] feature alternating $Co(1)O_6$ and $Co(2)O_6$ octahedra, where each $Co(1)O_6$ octahedron shares *trans* edges with two $Co(2)O_6$, and each $Co(2)O_6$ shares skew edges with one $Co(1)O_6$ and one $Co(2)O_6$. The fundamental building unit of the chain is $[Co_2(H_2O)_2(As_2O_7)_6]$. Units within one chain are related by *n*-glide symmetry operations. Adjacent chains which are related by 2_1 symmetry operations [Fig. 2(*b*)] are linked by the $As(2)O_4$ tetrahedra of the diarsenate groups to form wavy sheets parallel to the (101) plane (Fig. 3). As shown in Fig. 2(*b*), two types of windows are formed between adjacent chains in a sheet. One is an eight-membered ring of four CoO_6 octahedra and four tetrahedra of two diarsenate groups, and the other window is formed by two $Co(2)O_6$ octahedra and two $As(2)O_4$ tetrahedra. Infinite chains in neighbouring sheets are related by inversion centres. Adjacent sheets are connected by As_2O_7 groups in such a way that there are straight octagonal tunnels along [100] and tetragonal tunnels along [001]. All water hydrogen atoms are

Table 1 Crystallographic data for $Co_2As_2O_7(H_2O)_2$ and $Ni_2As_2O_7(H_2O)_2$[a]

Formula	$H_4As_2Co_2O_9$	$H_4As_2Ni_2O_9$
Colour	Purple	Pale green
M	415.74	415.25
a/Å	6.525(2)	6.459(2)
b/Å	14.200(5)	14.033(4)
c/Å	7.618(2)	7.543(2)
β/°	94.72(2)	94.24(2)
U/Å^3	703.4(4)	681.8(3)
D_c/g cm^{-3}	3.925	4.046
μ/cm^{-1}	140.77	151.80
$2\theta_{max}$/°	55.0	50.0
$R(F_o)$[b]	0.0246	0.0272
$R'(F_o)$[c]	0.0384	0.0307

[a] Details in common: space group $P2_1/n$, Z = 4, T = 23 °C and λ = 0.710 73 Å. [b] $R = \Sigma||F_o| - |F_c||/\Sigma|F_o|$. [c] $R' = [\Sigma w(|F_o| - |F_c|)^2/\Sigma w|F_o|^2]^{\frac{1}{2}}$, $w = [\sigma(F)^2 + gF^2]^{-1}$.

Table 2 Positional parameters for $Co_2As_2O_7(H_2O)_2$ and $Ni_2As_2O_7(H_2O)_2$

Atom	x	y	z
$Co_2As_2O_7(H_2O)_2$			
Co(1)	−0.042 89(8)	0.247 63(4)	0.643 75(7)
Co(2)	−0.261 82(8)	0.384 81(4)	0.913 75(7)
As(1)	0.442 70(6)	0.314 49(3)	0.559 68(5)
As(2)	0.238 56(6)	0.419 96(3)	0.849 09(5)
O(1)	0.654 1(4)	0.290 7(2)	0.693 0(4)
O(2)	0.481 3(5)	0.344 9(2)	0.354 2(4)
O(3)	0.266 4(4)	0.230 6(2)	0.584 4(4)
O(4)	0.334 7(4)	0.417 0(2)	0.640 2(4)
O(5)	0.176 8(4)	0.531 5(2)	0.874 3(4)
O(6)	0.430 2(4)	0.374 6(2)	0.981 8(4)
O(7)	0.031 4(4)	0.350 4(2)	0.839 0(4)
O(8)	−0.061 6(5)	0.343 8(2)	0.431 5(4)
O(9)	−0.255 1(5)	0.497 4(2)	0.737 1(4)
$Ni_2As_2O_7(H_2O)_2$			
Ni(1)	−0.040 93(14)	0.248 93(6)	0.642 88(12)
Ni(2)	−0.263 47(14)	0.382 70(6)	0.910 98(11)
As(1)	0.445 21(11)	0.313 78(50)	0.558 39(9)
As(2)	0.238 50(11)	0.420 52(5)	0.850 25(9)
O(1)	0.657 1(8)	0.287 2(4)	0.694 3(6)
O(2)	0.488 2(8)	0.345 4(3)	0.352 2(6)
O(3)	0.263 4(7)	0.229 4(3)	0.584 2(6)
O(4)	0.337 7(8)	0.417 7(3)	0.639 0(6)
O(5)	0.174 7(8)	0.533 5(3)	0.878 6(7)
O(6)	0.431 2(7)	0.373 2(3)	0.983 5(7)
O(7)	0.027 4(8)	0.350 1(4)	0.836 49(7)
O(8)	−0.058 2(9)	0.344 4(4)	0.4340(7)
O(9)	−0.258 4(4)	0.495 2(4)	0.735 2(7)

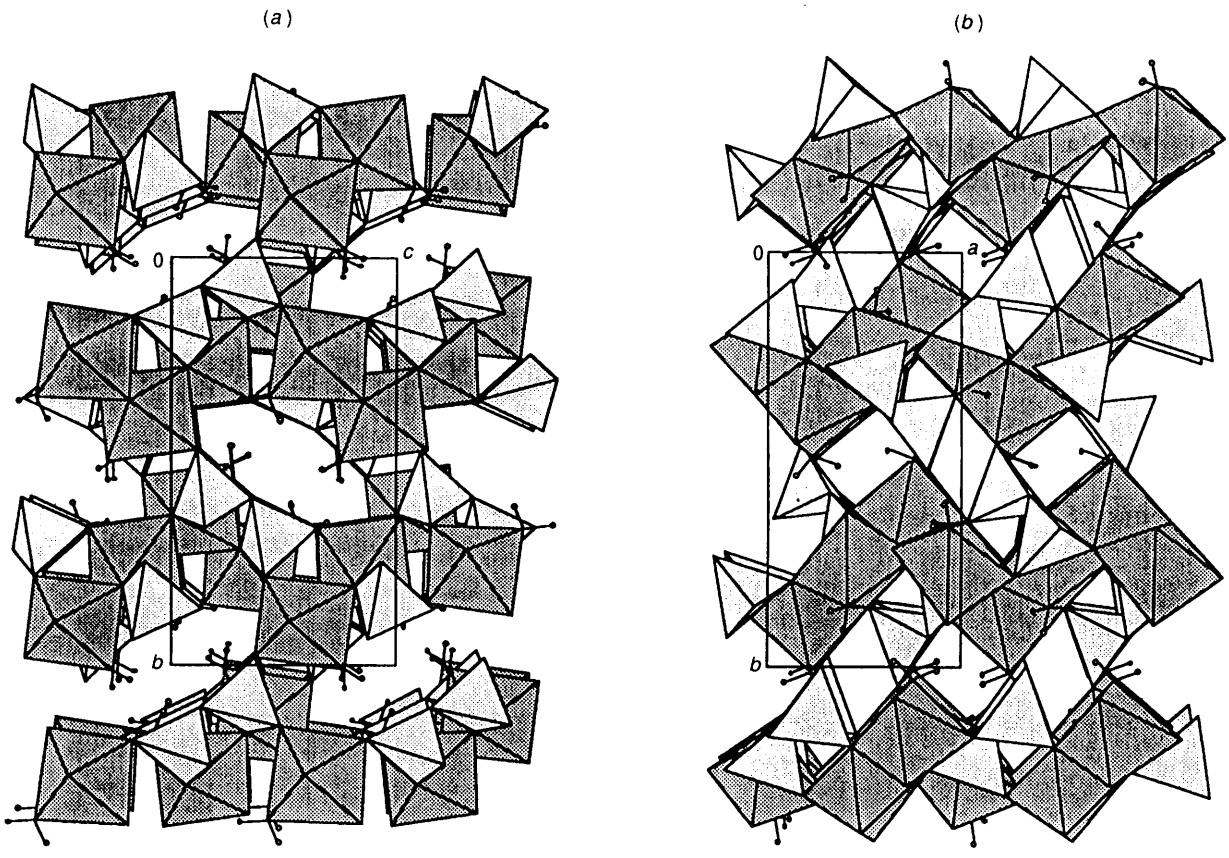

Fig. 1 Perspective view of the $Co_2As_2O_7(H_2O)_2$ structure along the [100] (*a*) and [001] (*b*) directions. In this representation the corners of octahedra and tetrahedra are O atoms and the Co and As atoms are at the centre of each octahedron and tetrahedron, respectively. The open circles are H atoms of water molecules

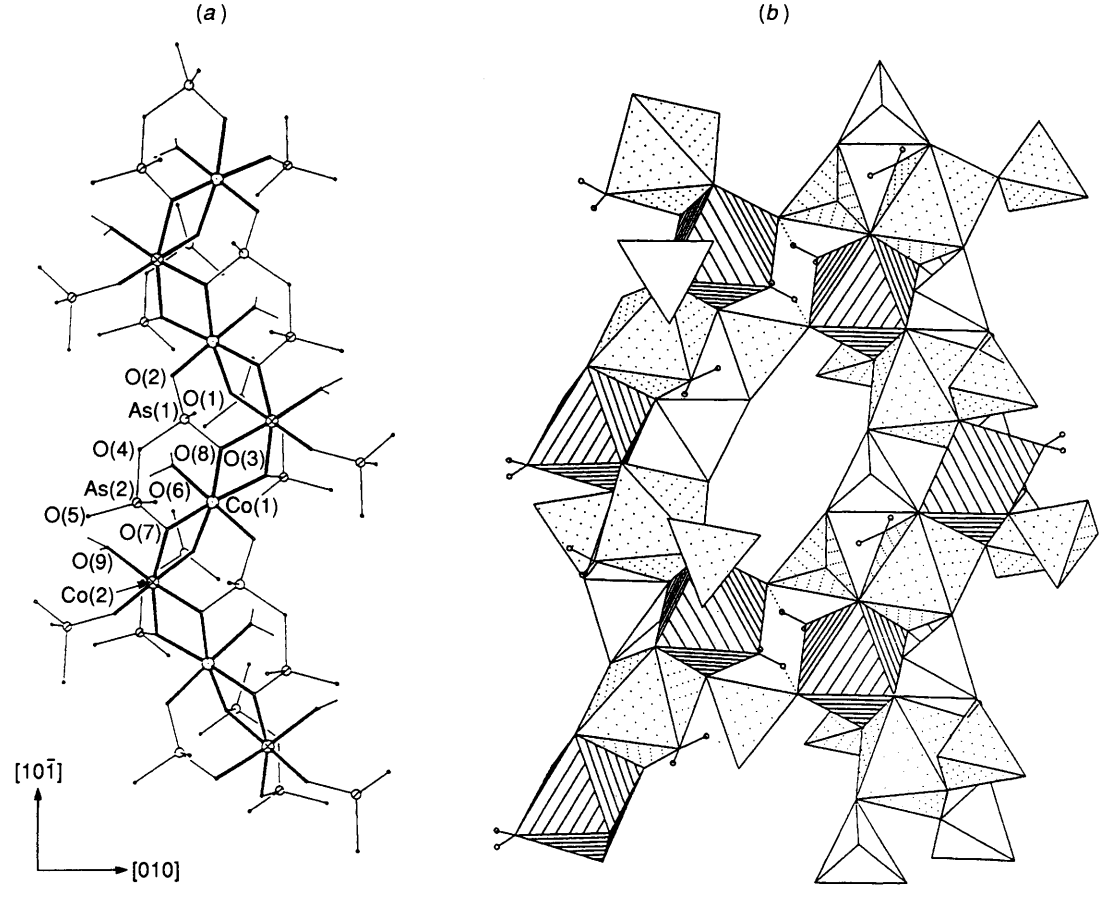

Fig. 2 Infinite chains in $Co_2As_2O_7(H_2O)_2$. (*a*) Ball and stick representation of a section of a zigzag chain. (*b*) Polyhedron representation of two adjacent chains projected onto the (101) plane. Interchain hydrogen bonds are shown as dotted lines

Table 3 Selected bond lengths (Å) and bond-valence sums (Σs) for $Co_2As_2O_7(H_2O)_2$ and $Ni_2As_2O_7(H_2O)_2$

$Co_2As_2O_7(H_2O)_2$		$Ni_2As_2O_7(H_2O)_2$	
Co(1)–O(1^{I})	2.132(3)	Ni(1)–O(1^{I})	2.087(5)
Co(1)–O(2^{II})	2.068(3)	Ni(1)–O(2^{II})	2.058(5)
Co(1)–O(3)	2.118(3)	Ni(1)–O(3)	2.065(5)
Co(1)–O(6^{II})	2.129(3)	Ni(1)–O(6^{II})	2.093(5)
Co(1)–O(7)	2.112(3)	Ni(1)–O(7)	2.060(5)
Co(1)–O(8)	2.113(3)	Ni(1)–O(8)	2.065(6)
Σs[Co(1)–O] = 1.93		Σs[Ni(1)–O] = 1.94	
Co(2)–O(1^{I})	2.182(3)	Ni(2)–O(1^{I})	2.146(5)
Co(2)–O(3^{III})	2.090(3)	Ni(2)–O(3^{III})	2.045(5)
Co(2)–O(5^{IV})	2.045(3)	Ni(2)–O(5^{IV})	2.024(5)
Co(2)–O(6^{I})	2.121(3)	Ni(2)–O(6^{I})	2.089(5)
Co(2)–O(7)	2.098(3)	Ni(2)–O(7)	2.052(5)
Co(2)–O(9)	2.092(3)	Ni(2)–O(9)	2.064(6)
Σs[Co(2)–O] = 1.98		Σs[Ni(2)–O] = 1.96	
As(1)–O(1)	1.679(3)	As(1)–O(1)	1.690(5)
As(1)–O(2)	1.663(3)	As(1)–O(2)	1.660(5)
As(1)–O(3)	1.677(3)	As(1)–O(3)	1.689(5)
As(1)–O(4)	1.750(3)	As(1)–O(4)	1.744(5)
Σs[As(1)–O] = 4.92		Σs[As(1)–O] = 4.87	
As(2)–O(4)	1.758(3)	As(2)–O(4)	1.761(5)
As(2)–O(5)	1.649(3)	As(2)–O(5)	1.656(5)
As(2)–O(6)	1.671(3)	As(2)–O(6)	1.678(5)
As(2)–O(7)	1.671(3)	As(2)–O(7)	1.681(5)
Σs[As(2)–O] = 5.02		Σs[As(2)–O] = 4.90	
O(8)–H(8A)	1.02	O(8)–H(8A)	0.93
O(8)–H(8B)	0.84	O(8)–H(8B)	0.92
O(9)–H(9A)	0.99	O(9)–H(9A)	0.96
O(9)–H(9B)	0.83	O(9)–H(9B)	1.01
O(2)···H(9B^{V})	2.061	O(2)···H(9B^{V})	1.740
O(5)···H(8B)	2.187	O(5)···H(8B^{V})	2.293
O(5)···H(9A)	2.419	O(5)···H(9A)	2.120
O(2)···O(9^{V})	2.741	O(2)···O(9^{V})	2.739
O(5)···O(8^{V})	2.973	O(5)···O(8^{V})	2.967
O(5)···O(9)	2.964	O(5)···O(9)	2.973
Co(1)···Co(2)	3.248	Ni(1)···Ni(2)	3.180
Co(1)···Co(2^{IV})	3.240	Ni(1)···Ni(2^{IV})	3.185

Symmetry codes: I $x-1, y, z$; II $x-\frac{1}{2}, \frac{1}{2}-y, \frac{1}{2}+z$; III $\frac{1}{2}+x, \frac{1}{2}-y, \frac{1}{2}+z$; IV $-x, 1-y, 2-z$; V $-x, 1-y, 1-z$.

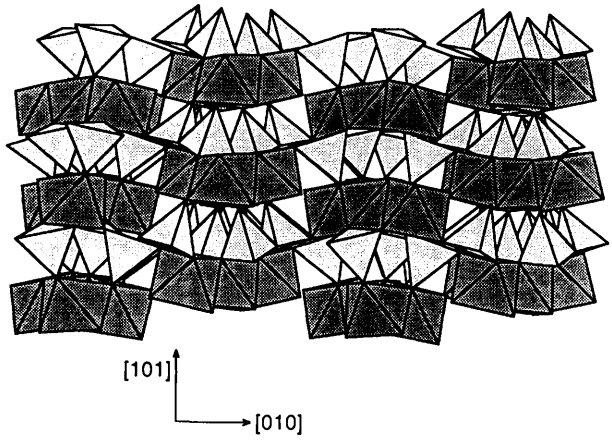

Fig. 3 Wavy sheets in the structure of $Co_2As_2O_7(H_2O)_2$. View along the [10$\bar{1}$] direction

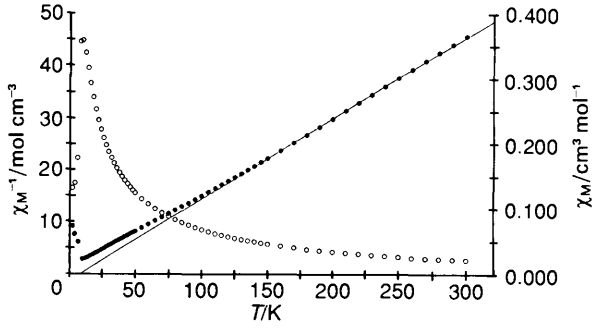

Fig. 4 Magnetic susceptibility (χ_M, ○) and inverse magnetic susceptibility (χ_M^{-1}, ●) plotted as a function of temperature for a powder sample of $Co_2As_2O_7(H_2O)_2$

directed into the [100] tunnel, while half of them [H(9A) and H(9B)] are also directed into the [001] tunnel. Thus, the latter hydrogen atoms are at the intersections of these tunnels. Linkage between adjacent chains also involves hydrogen bonds. The O(5)···O(9) distance (2.964 Å) represents weak hydrogen bonding between adjacent chains within a sheet and O(2)···O(9) (2.741 Å) a stronger hydrogen bonding between adjacent sheets.

Infinite chains of CoO_6 octahedra sharing both skew and *trans* edges were also observed in a recently discovered cobalt diphosphate, $CaCo_3(P_2O_7)_2$,[14] but these chains are apparently different in terms of symmetry and width. In the calcium compound, each infinite chain contains a symmetry of inversion with a zigzag step of one octahedron wide, whereas there are *n*-glide symmetry operations within a chain and the step is two octahedra wide in $Co_2As_2O_7(H_2O)_2$. The difference is also attributed to the different connectivity of the P_2O_7 and As_2O_7 groups to the polyhedra connections in the structures. In $CaCo_3(P_2O_7)_2$, the two tetrahedra of a P_2O_7 group are linked to seven CoO_6 octahedra and are in a semi-eclipsed configuration with P–O–P 135.3°. In $Co_2As_2O_7(H_2O)_2$, however, each diarsenate group is linked to eight octahedra and the two tetrahedra are in a nearly eclipsed configuration with As–O–As 121.4°. Each As_2O_7 group shares its six oxygen atom vertices with four octahedra [two $Co(1)O_6$ and two $Co(2)O_6$] within a chain, one $Co(2)O_6$ in an adjacent chain, and two $Co(1)O_6$ and one $Co(2)O_6$ of a neighbouring sheet. Both CoO_6 octahedra are distorted and the distortion can be estimated by using the equation $\Delta = 1/6\Sigma[(R_i - \bar{R})/\bar{R}]^2$, where R_i = an individual bond length and $\bar{R}$ = an average bond length.[15] The calculation results indicate that the distortion in $Co(2)O_6$ is more pronounced than that in $Co(1)O_6$ ($10^4\Delta$ = 3.85 *vs.* 0.99; 3.59 *vs.* 0.43 in the nickel compound). The greater distortion in $Co(2)O_6$ [or $Ni(2)O_6$] is due to skew edge-sharing.

Fig. 4 shows the magnetic susceptibility and inverse magnetic susceptibility of $Co_2As_2O_7(H_2O)_2$ plotted as a function of temperature. The data above 125 K can be described well by the Curie–Weiss equation $\chi_M = C/(T - \theta)$ where C = 6.41 cm^3 K mol^{-1} and θ = 8.29 K. From the relation $C = N\mu_{eff}^2/3k_B$ one obtains the effective magnetic moment μ_{eff} per metal atom equal to 5.06 μ_B ($\mu_B \approx 9.274 \times 10^{-24}$ J T^{-1}). These results indicate that $Co_2As_2O_7(H_2O)_2$ is paramagnetic between 125 and 300 K with an effective magnetic moment expected for a high-spin cobalt(II) compound. Below 125 K the magnetic susceptibility gradually rises to a maximum at *ca.* 10 K and then decreases sharply. This maximum is attributed to antiferromagnetic interactions between the cobalt atoms.

In the TG measurement, the weight loss occurs at *ca.* 420 °C, indicative of tightly bound water molecules. This is consistent with the structural analysis result, showing that the water oxygen is co-ordinated to the cobalt atoms.

Acknowledgements

Support for this study by the National Science Council of the Republic of China is gratefully acknowledged.

References

1 (*a*) E. Dvoncova and K.-H. Lii, *Inorg. Chem.*, 1993, **32**, 4368; (*b*) R. C. Haushalter, Z. Wang, M. E. Thomson, J. Zubieta and C. J. O'Connor, *Inorg. Chem.*, 1993, **32**, 3966; (*c*) P. Crespoa, A. Grandin, M. M. Borel, A. Leclaire and B. Raveau, *J. Solid State Chem.*, 1993, **105**, 307; (*d*) T. M. Nenoff, W. T. A. Harrison, T. E. Gier, J. C. Calabrese and G. D. Stucky, *J. Solid State Chem.*, 1993, **107**, 285.

2 S.-L. Wang and W.-C. Lee, *Acta Crystallogr., Sect. C*, 1991, **47**, 1709.

3 C.-Y. Cheng and S.-L. Wang, *J. Chem. Soc., Dalton Trans.*, 1992, 2395.

4 S.-L. Wang and C.-Y. Cheng, *J. Solid State Chem.*, 1994, **109**, 277.

5 S.-L. Wang, C.-H. Wu and S.-N. Liu, *J. Solid State Chem.*, in the press.

6 W. T. A. Harrison, T. E. Gier and G. D. Stucky, *Eur. J. Solid State Inorg. Chem.*, 1993, **30**, 761.

7 A. M. Buckley, S. T. Bramwell and P. Day, *J. Solid State Chem.*, 1990, **86**, 1.

8 M. A. G. Aranda, S. Bruque and J. P. Attfield, *Inorg. Chem.*, 1991, **30**, 2043.

9 G. M. Sheldrick, SHELXTL PLUS Crystallographic System, release 4.21, Siemens Analytical X-Ray Instruments, Madison, WI, 1991.

10 P. W. Selwood, *Magnetochemistry*, Interscience, New York, 1956.

11 I. D. Brown and D. Altermatt, *Acta Crystallogr., Sect. B*, 1985, **41**, 244.

12 D. W. J. Cruickshank, H. Lynton and G. A. Barclay, *Acta Crystallogr.*, 1962, **15**, 491.

13 N. Krishnamachari and C. Calvo, *Acta Crystallogr., Sect. B*, 1972, **28**, 2883.

14 K. H. Lii, P. F. Shih and T. M. Chen, *Inorg. Chem.*, 1993, **32**, 4373.

15 R. D. Shannon, *Acta Crystallogr., Sect. A*, 1976, **32**, 751.

Received 21*st December* 1993; *Paper* 3/07502H